

Heat capacity of liquid ^3He in sintered silver powder

S. Kishishita,* H. Kambara,[†] and T. Mamiya

Department of Physics, Nagoya University, Chikusa-ku, Nagoya 464-8602, Japan

(Received 29 May 2000; published 20 December 2000)

We have measured the heat capacity of liquid ^3He in silver sinter at pressures from 0 MPa up to 3.31 MPa and in the temperature range from about 1 up to 28 mK. The heat capacity in the normal fluid is found to be the sum of the heat capacity of bulk normal fluid and a temperature-independent heat capacity ΔC due to amorphous solid layers on the silver sinter surface, where $\Delta C = 7.3 \pm 6.8 \mu\text{J K}^{-1} \text{m}^{-2}$ corresponds to 1 ± 1 amorphous solid layers. This value is in rough agreement with other results, including solid ^3He and ^3He adsorbed on Vycor and silver sinter, and differs from the value for liquid ^3He in silver sinter reported by Schrenk and König. Our result indicates that the amorphous solid layers on a large surface area yield a universal ΔC in unit area throughout liquid, solid, and adsorbed ^3He in contact with a large surface. The superfluid transition temperature of the liquid ^3He in the silver sinter is in good agreement with the theory of Kjälldman and Kurkijärvi when taking the pore diameter to be 3400 Å, and our observations differ from the results of Schrenk and König.

DOI: 10.1103/PhysRevB.63.024512

PACS number(s): 67.55.Cx, 67.57.Bc

I. INTRODUCTION

Recent studies have proposed the question of whether excess heat capacity exists as well as the normal bulk heat capacity, when liquid and solid ^3He are in contact with a large surface area. Kambara *et al.* observed the excess heat capacity in addition to the specific heat due to the multiple-spin-exchange interaction in bcc solid ^3He .¹ They concluded that the excess heat capacity originated from the amorphous solid layers on the inhomogeneous silver surface. Golov and Pobell found the temperature-independent heat capacity as well as the heat capacity of normal liquid ^3He in the Vycor glass.² Greywall and Busch found a similar excess heat capacity for liquid ^3He in the silver sinter.³ Golov and Pobell suggested that the excess constant heat capacity of $13 \mu\text{J/Km}^2$ for the substrate of the Vycor and silver sinter is due to the amorphous solid layers on the inhomogeneous surfaces.² In contrast to the past results Schrenk and König reported the new result that the constant heat capacity in the silver sinter is several times as large as the constant heat capacity in the Vycor glass.⁴ They presented new issues of whether the constant heat capacity depends on the substrate, i.e., silver or Vycor, and whether it depends on liquid or solid. We intend to resolve these issues by measuring the heat capacity for both the liquid and solid ^3He on the same substrate. Our results are interpreted in terms of a constant heat capacity arising from a common origin.

II. EXPERIMENTAL CONFIGURATION

Calorimetry was performed with the adiabatic heat-pulse method. The cell chamber and thermal link were made primarily of pure silver. We used a fine silver powder,⁵ nominally 700 Å in diameter, by packing it to 48% in order to get good thermal conduction to the sample. The entire volume of the sample was 1.77 cm^3 , and the total surface area in the cell was determined to be 21 m^2 from the nitrogen BET adsorption measurement. These quantities yielded an average pore diameter in the sinter of approximately 3400 Å

using the method of Robertson *et al.*⁶ The Pt-NMR and RuO_2 resistance thermometers used for the calorimeter were calibrated against a ^3He melting curve thermometer.⁷ The calorimeter was attached to a nuclear demagnetization stage of copper via a thermal switch of tin. The measurements were done in the temperature range from 1 up to 28 mK and at pressures of liquid ^3He from 0 up to 3.31 MPa. The net specific heat was obtained by subtracting the heat capacity of the addenda from the total heat capacity.

III. HEAT CAPACITY OF NORMAL PHASE

The results for the heat capacity of seven samples of liquid ^3He at pressures from 0 MPa (saturated vapor pressure, $36.84 \text{ cm}^3/\text{mol}$) to 3.31 MPa ($25.73 \text{ cm}^3/\text{mol}$) are shown in Fig. 1. The solid lines in Fig. 1 indicate the Greywall's bulk liquid data⁸ corrected for the pressures in the present samples. At low temperatures there are distinct jumps due to the second order transition from the superfluid to normal phase, except for the 0 MPa sample. First, we will discuss the heat capacity of normal phase.

At very low temperatures ($T \ll T_F$), the heat capacity for the degenerate Fermi gas is linear in T as given by

$$C = \frac{\pi^2 R T}{2 T_F} \quad (1)$$

with

$$T_F = \frac{\hbar^2}{2 m_3 k_B} \left(\frac{3 \pi^2 N_A}{V_m} \right)^{2/3}, \quad (2)$$

where T_F is the Fermi temperature, R is the gas constant, k_B is the Boltzmann constant, \hbar is Planck's constant divided by 2π , m_3 is the mass of ^3He atom, N_A is Avogadro's number, and V_m is the molar volume.

According to the Landau theory, which treats ^3He as a Fermi liquid, ^3He - ^3He interactions modify the heat capacity only through the renormalization of the ^3He mass.⁹ In other words, Eq. (2) holds with the mass m_3 replaced with an

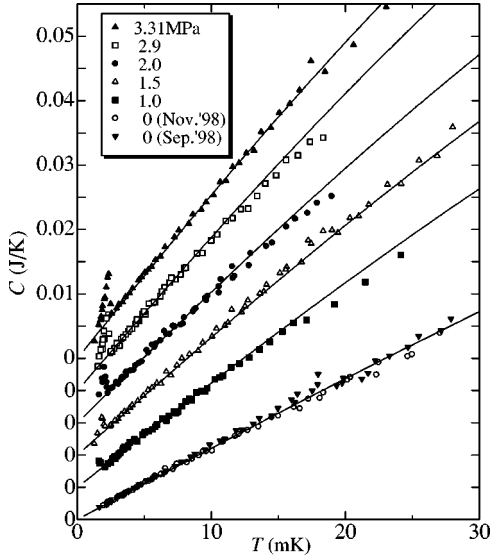


FIG. 1. The results for the heat capacity of seven samples of liquid ^3He at molar volumes from $25.73 \text{ cm}^3/\text{mol}$ (3.31 MPa) to $36.84 \text{ cm}^3/\text{mol}$ (0 MPa or saturated vapor pressure) are shown. Note that zero is shifted for each sample for clarity. The solid line indicates the bulk liquid data corrected to the sample pressure.

effective mass m_3^* . The temperature dependence of the heat capacity of the normal liquid ^3He ($C \propto T$) is the same as that of the perfect Fermi gas in this degenerate region. Meanwhile, the original Landau formulation which was extended to higher temperatures by including the effects of spin fluctuation or paramagnons was confirmed experimentally up to about 100 mK (Refs. 8,10) as represented by the following equation:

$$C = \gamma RT + \Gamma RT^3 \ln\left(\frac{T}{\Theta_c}\right), \quad (3)$$

where γ , Γ and Θ_c are the constant values which depend on the sample pressure. Furthermore, Golov and Pobell proposed the presence of a constant heat capacity based on the assumption that the density of the number of spins is constant as a function of the logarithm of the exchange interaction in the first two layers of the amorphous solid due to the rough substrate as in the case of Vycor glass or silver sinter.²

When fitting the data to the equations for specific heat, it is desirable to analyze a temperature region as low as possible in order to obtain the precise γ and ΔC , the constant heat capacity, through the use of

$$C = nR\gamma_s T + \Delta C, \quad (4)$$

where γ_s (K^{-1}) and ΔC (J K^{-1}) are the fitting parameters, and n is the number of moles in the sample cell (See Fig. 2). Note that C is now measured in J K^{-1} , where the suffix s expresses the silver sinter. However, we found that the number of our data points was too small to obtain the precise values for the parameters partly because of the inevitable experimental scatter and partly because the minimum temperature is limited by the onset of the superfluid transition. Consequently, we had to analyze a wider temperature region

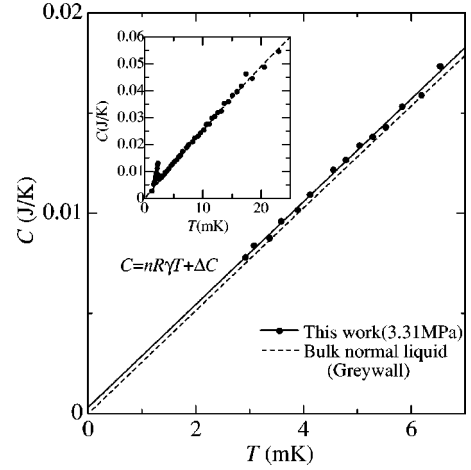


FIG. 2. An example of fitting the data points to Eq. (4) is shown for the sample at 3.31 MPa. The inset shows the entire diagram including superfluid state. The difference between the solid line and dotted line shows the presence of ΔC .

that included data at higher temperatures. We fit our data with Eq. (4) in the temperature range extended up to a high-temperature limit T_{hi} as defined by

$$\left| nR\Gamma T_{\text{hi}}^3 \ln\left(\frac{T_{\text{hi}}}{\Theta_c}\right) \right| = \frac{1}{2} \Delta C. \quad (5)$$

This limit indicates that one takes the temperature range with less effect of the second term of Eq. (3) than the ΔC term in Eq. (4). This procedure leads to taking a sufficient number of data points with the temperature range as low as possible in order to obtain a more precise ΔC . Equation (5) provides the criterion common to all the samples for taking the proper temperature range, and thus the temperature region for the fit extends from T_{low} , the superfluid transition temperature, up to T_{hi} . This procedure makes γ_s 1% smaller and ΔC 15% larger than the Greywall's values.⁸ We neglected the differences of this amount in these parameters because it turned out that the experimental uncertainties for γ_s and ΔC in the present study are larger than these differences. We substituted the Greywall's values for Γ and Θ_c and $13 \mu\text{J K}^{-1} \text{m}^2$ for ΔC in the Eq. (5), only to estimate T_{hi} , which is listed for each sample in Table I.

The coefficients obtained from the present data are given in Table I. Pressure dependence of linear coefficients for the heat capacity of seven samples of liquid ^3He are shown in Fig. 3. For comparison, the γ_s values reported by Schrenk and König⁴ are also plotted in Fig. 3. The solid line represents the data of bulk liquid ^3He obtained by Greywall.⁸ The present γ_s values agree with the value of γ for bulk liquid, which indicates that there is no effect of restricted geometry on the heat capacity of the liquid in the silver pores of 3400 \AA in diameter. The fact that there is no effect of restricted geometry was also reported by Golov and Pobell² for the case of Vycor glass with a pore size 70 \AA . The characteristic length of normal fluid ^3He is the de Broglie wavelength λ of a quasiparticle of about 8 \AA . If the dimension of confinement is much larger than the de Broglie wavelength,

TABLE I. The coefficients obtained from the data. P is the pressure of the liquid ^3He . V is molar volume. γ_s and ΔC are the linear coefficient in temperature and the constant heat capacity, respectively. T_{hi} is the temperature defined by Eq. (5), where fitting was done in the temperature range between the lowest temperature and T_{hi} .

P (MPa)	V (cm ³ /mol)	γ_s (K ⁻¹)	ΔC ($\mu\text{J K}^{-1} \text{m}^{-2}$)	T_{hi} (mK)
0 (1st)	36.84	2.87 ± 0.02	-0.77 ± 3.4	14
0 (2nd)	36.84	2.70 ± 0.03	13 ± 3.9	14
1.0	30.35	3.25 ± 0.04	14 ± 5.3	9.6
1.5	28.89	3.62 ± 0.07	6.6 ± 8.4	8.7
2.0	27.75	3.85 ± 0.07	7.1 ± 9.5	8.0
2.9	26.29	4.35 ± 0.07	-4.4 ± 9.0	7.0
3.31	25.73	4.48 ± 0.06	15 ± 8.1	6.7

Fermi liquid theory should be valid and leads to no effects of restricted geometry, which is in agreement with our results. The γ_s in the silver sinter obtained by Schrenk and König⁴ was larger by about 20%, compared with all other results including the present study, the result for Vycor glass² and Greywall's bulk value γ .⁸ We will discuss the possible origin of the discrepancy of γ_s value in the next section.

The pressure dependence of temperature-independent heat capacity ΔC in unit area for seven samples of liquid ^3He are shown in Fig. 4. For comparison, ΔC obtained by Schrenk and König⁴ is also plotted. We have found that our ΔC is pressure independent and its magnitude is $7.3 \pm 6.8 \mu\text{J K}^{-1} \text{m}^{-2}$. Within the uncertainty limit this value is consistent with $\approx 10 \mu\text{J K}^{-1} \text{m}^{-2}$ reported for Vycor glass. The temperature-independent heat capacity is expressed by Golov and Pobell² as

$$\Delta C = k_B \ln 2 \frac{N_0}{\ln(T_h/T_l)}, \quad (6)$$

where N_0 is the total number of spins in the amorphous solid on silver surface, and its ordering temperature T_c is distrib-

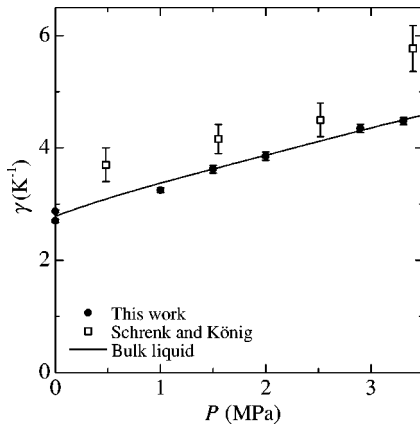


FIG. 3. Pressure dependence of the linear coefficient, γ_s , for the heat capacity of seven samples of liquid ^3He . For comparison, γ_s obtained by Schrenk and König (Ref. 4) is also plotted. The solid line represents the data of bulk liquid ^3He obtained by Greywall (Ref. 8).

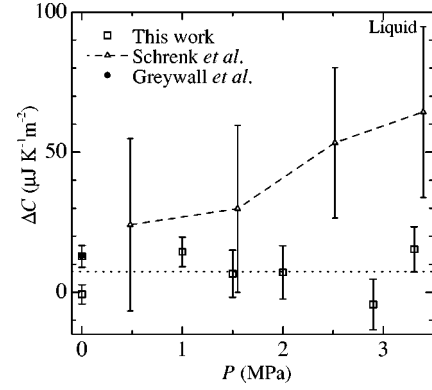


FIG. 4. Pressure dependence of the constant heat capacity ΔC in a unit area for seven samples of liquid ^3He . For comparison the temperature-independent heat capacity obtained by Schrenk and König (Ref. 4) and the heat capacity of the thin film on the surface of silver sinter at saturated vapor pressure obtained by Greywall and Busch (Ref. 3) are also plotted. The dotted line represents ΔC averaged over all samples.

uted between T_l and T_h . Substituting $\Delta C = 7.3 \pm 6.8 \mu\text{J K}^{-1} \text{m}^{-2}$, $T_h = 40 \text{ mK}$, and $T_l = 1.5 \mu\text{K}^2$ for Eq. (6), we have estimated the amorphous solid layers by using a coverage of 11 atoms/nm² for the first layer and 8 atoms/nm² for the second layer.³ Comparing experimental values² with theoretical values obtained from Eq. (6), we note that the number of amorphous layers obtained from Eq. (6) is 1.6 times as large as those obtained from experiment. By taking this factor into account for the present ΔC value, we obtain a coverage of about 12 atoms/nm², which corresponds to the presence of about 1 ± 1 layers of the amorphous solid. Our result is consistent with the work of Golov and Pobell² who have obtained a coverage of 17.2 atoms/nm², which corresponds to the presence of 1.8 layers of amorphous solid. Meanwhile, the magnitude of ΔC obtained by Schrenk and König is about 7 times as large as the magnitude obtained by us. We will discuss this discrepancy in a later section. We note that Schuhl *et al.* reported an increase of 60% of adsorbed solid on the surface of teflon particles in the liquid at 3.2 MPa compared to 0.046 MPa.¹¹

Finally, we comment on the constant specific heat for solid ^3He in contact with silver sinter. ΔC throughout the liquid state in the present work and the solid state in the previous work¹ is shown in Fig. 5. The average value of ΔC in the solid state is $12.1 \pm 3.1 \mu\text{J K}^{-1} \text{m}^{-2}$ which corresponds to 1.7 ± 0.6 layers and is larger than the the average value of $\Delta C = 7.3 \pm 6.8 \mu\text{J K}^{-1} \text{m}^{-2}$ in the liquid state. We note that ΔC in solid state is more precise than that in liquid state because the ratio of $\Delta C/C$ in the solid state is 30% compared to 6% in the liquid state, if we take the largest percent in each state. The simple average of ΔC over the entire pressure range including both states is $9.0 \mu\text{J K}^{-1} \text{m}^{-2}$. We believe that the real value of ΔC should be close to the value in the solid state and should be common to both states.

IV. HEAT CAPACITY OF SUPERFLUID PHASE

The temperature dependence of the heat capacity of superfluid ^3He for 3.31 MPa is shown in Fig. 6. For compari-

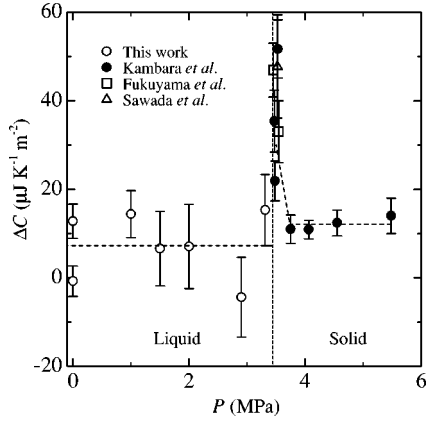


FIG. 5. Pressure dependence of the constant heat capacity ΔC throughout liquid and solid state of ^3He in contact with the silver sinter. The dashed vertical line shows the boundary between the liquid and solid phases. The data of Kambara *et al.* (Ref. 1), Fukuyama *et al.* (Ref. 13), and Sawada *et al.* (Ref. 14) are also shown.

son, the data of bulk superfluid⁷ and the data in the silver sinter obtained by Schrenk and König⁴ are represented together. Here T_s^i marks the temperature for the onset of superfluid transition and T_s^{\max} is the temperature at which heat capacity has its maximum value. As in the data obtained by Schrenk and König, we do not observe a sharp peak but a broad one in the heat capacity of ^3He in the silver sinter. The magnitude of the heat capacity at T_s^{\max} is smaller than the value obtained in bulk ^3He at its transition temperature T_c . The reason for a broad peak in the superfluid transition is as follows. The transition temperature is effected by the pore size; the smaller the pore, the lower the T_c . The distribution of the pore sizes in the sinter then leads to a different transition temperature range $T_s^{\max} < T < T_s^i$ because the coherence length of the superfluid is of the same order as the pore size. This means that the diameter of the pore is considered to have a distribution central around 3400 Å.

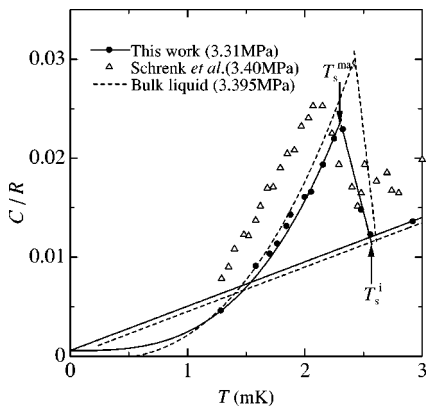


FIG. 6. Temperature dependence of the heat capacity of superfluid ^3He for 3.31 MPa. For comparison the data of bulk superfluid (Ref. 7) (dashed line) and the data in the silver sinter obtained by Schrenk and König (triangles) are displayed together. T_s^i marks the onset of superfluid transition and T_s^{\max} is the temperature at which heat capacity has its maximum value. We have decided that the superfluid transition temperature T_s^m is the average of T_s^i and T_s^{\max} .

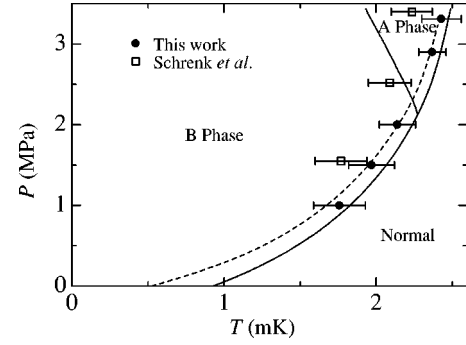


FIG. 7. The pressure dependence of the superfluid transition temperature. For comparison the data of bulk liquid (Ref. 7) (solid line) and the data obtained by Schrenk and König (Ref. 4) (squares) are also displayed. The superfluid transition temperature calculated for a pore size of 3400 Å following the description provided by Kjälman and Kurkijärvi, is shown with a dashed line.

Kjälman and Kurkijärvi have calculated the suppression of the transition temperature of superfluid ^3He as a function of the size of an infinitely long cylindrical pore with diffusely scattering walls.¹² We decided that the proper phase transition temperature T_s^m in the silver sinter is the average of T_s^i and T_s^{\max} , except for the sample at 0 MPa, which did not show evidence of superfluidity. The relation between the superfluid transition temperature and the sample pressure is shown in Fig. 7. For comparison, the data of bulk liquid and the data obtained by Schrenk and König⁴ are displayed together. In addition, the calculated result for the pore size of 3400 Å when using the theory of Kjälman and Kurkijärvi, is shown with a dashed line. The left and right sides of the error bar are T_s^{\max} and T_s^i , respectively, and the middle point T_s^m is taken to be the average superfluid transition temperature in the silver sinter. The present T_s^m values agree with the theoretical predictions as seen in Fig. 7, but the data of Schrenk and König, when analyzed in the same manner, deviate largely from our results.

We derived the superfluid fraction n in liquid ^3He on the assumption that the specific heat of the superfluid ^3He in the sinter has the same temperature dependence as bulk ^3He .⁷ The superfluid fraction in the present study is about 80% in contrast with about 60% in the results of Schrenk and König,⁴ as shown in Table II. The smaller superfluid fraction for Schrenk and König is assumed to come partially from the

TABLE II. Transition temperatures of liquid ^3He in the silver sinter. P is the pressure of the sample. ξ_0 is the coherence length. n is the superfluid fraction of liquid ^3He . T_s^m is the average superfluid transition temperature in the pores of the silver sinter.

P (MPa)	ξ_0 (Å)	n (%)	T_s^m (mK)
0	780		
1.0	310		1.76
1.5	250		1.97
2.0	210	80	2.14
2.9	170	77	2.37
3.31	160	75	2.43

larger γ values in their results. We note that this analysis gives only the measure of the effective superfluid fraction since the order parameter of the superfluid in the restricted geometry is different from the order parameter in bulk superfluid.¹²

Incidentally, the pore diameter of the sample cell of Schrenk and König is estimated to be 2900 Å, when applying Robertson's method⁶ and using the values of the surface area 52 m² and sample volume 3.72 cm³. This pore size contrasts with the 1000 Å value used in their paper. If we calculate their pore size correctly, their T_s^m must be plotted on the theoretical line (dashed line). Since the pore sizes of 2900 and 3400 Å give approximately the same effect on the superfluid transition temperature, the large depression in their superfluid transition temperature must be explained in a different way. We suppose that their temperature scale is 10% lower than the correct temperature scale over the entire temperature range of their measurement. Although their sample at 1.55 MPa showed a transition temperature of 1.8 mK, it should have the temperature of 2.0 mK. This proposed shift in their temperature scale also leads to the apparent enhancement of their γ_s values by 20% more than the known values.

V. SUMMARY

We have studied the heat capacity of liquid ^3He in a silver sinter in the restricted geometry at pressures from 0 up

to 3.31 MPa and in the temperature range from about 1 up to 28 mK. The heat capacity in the normal fluid can be interpreted as the sum of the heat capacity of bulk normal fluid and a temperature-independent heat capacity due to amorphous solid layers on the silver sinter surface. There is no significant difference between the heat capacity of liquid ^3He in the silver sinter and that of bulk normal liquid, except for the existence of the temperature-independent heat capacity in the former. Concerning the temperature-independent heat capacity, we have obtained the result that its magnitude is $7.3 \pm 6.8 \mu\text{J K}^{-1} \text{m}^{-2}$, which corresponds to 1 ± 1 layers of amorphous solid, and that it is independent of pressure in the liquid phase. With experimental error our value is in agreement with the value obtained by Golov and Pobell on the Vycor glass. The superfluid transition temperatures in the present study agree with the theoretical predictions for pores of 3400 Å.

ACKNOWLEDGMENTS

We are grateful to R. König and T. Mastushita for critical discussions and to M. Saitoh, W. Itoh, and T. Kurokawa for technical support. We are also thankful to M. W. Meisel for reading the manuscript. This work was supported by a Grant-in-Aid for International Scientific Research Program from the Ministry of Education, Science and Culture of Japan.

*Present address: Inasa Senior High School, 1428 Kanasashi, Inasa-cho, Shizuoka 431-2213, Japan.

†Present address: Department of Physics, Graduate School of Science, University of Tokyo, 7-3-1 Hongo, Bunkyo-ku, Tokyo 113-0033, Japan.

¹H. Kambara, S. Kishishita, T. Matsushita, and T. Mamiya, *Europhys. Lett.* **46**, 499 (1999). H. Kambara, S. Kishishita, and T. Mamiya, *Physica B* **284-288**, 204 (2000).

²A. Golov and F. Pobell, *Phys. Rev. B* **53**, 12 647 (1996); *Europhys. Lett.* **38**, 353 (1997).

³D.S. Greywall and P.A. Busch, *Phys. Rev. Lett.* **60**, 1860 (1988).

⁴R. Schrenk and R. König, *Phys. Rev. B* **57**, 8518 (1998).

⁵Ag powder: Vacuum Metallurgical Co., Ltd. 516 Yokota, Yamatake-cho, Chiba 289-1226, Japan.

⁶R.J. Robertson, F. Guillon, and J.P. Harrison, *Can. J. Phys.* **61**, 164 (1983). A factor (1- p) in Eq. (3) in this reference is mis-

leading and should be deleted.

⁷D.S. Greywall, *Phys. Rev. B* **33**, 7520 (1986).

⁸D.S. Greywall, *Phys. Rev. B* **27**, 2747 (1983).

⁹L.D. Landau, *Zh. Éksp. Teor. Fiz.* **30**, 1055 (1956) [*Sov. Phys. JETP* **3**, 920 (1957)].

¹⁰G. Baym and C. J. Pethick, in *The Physics of Liquid and Solid Helium*, edited by K. H. Bennemann and B. Ketterson (Wiley, New York, 1978), P. II.

¹¹A. Schuhl, S. Maegawa, M.W. Meisel, and M. Chapellier, *Phys. Rev. B* **36**, 6811 (1987).

¹²L.H. Kjåldman and J. Kurkijärvi, *J. Low Temp. Phys.* **33**, 577 (1978).

¹³H. Fukuyama, Y. Miwa, A. Sawada, and Y. Masuda, *J. Phys. Soc. Jpn.* **53**, 916 (1984).

¹⁴A. Sawada, H. Yano, M. Kato, K. Iwahashi, and Y. Masuda, *Phys. Rev. Lett.* **56**, 1587 (1986).